Predicting the Bond Behavior of Prestressed Concrete Beams Containing Debonded Strands

Bruce W. Russell Ph.D., P.E.
Assistant Professor
School of Civil Engineering and Environmental Science
University of Oklahoma
Norman, Oklahoma

Ned H. Burns, Ph.D., P.E.
Director, Ferguson Structural Engineering Laboratory
Zarrow Centennial Professor of Engineering
The University of Texas at Austin
Austin, Texas

Leslie G. ZumBrunnen
Project Engineer
Law Engineering, Inc.
Austin, Texas

Static flexural tests were performed on prestressed concrete beam specimens made with debonded strands. A behavioral model based on the prediction of cracking in regions of the transfer zone of debonded strands was used to predict strand anchorage failures. Agreement between the test results and the prediction is excellent, demonstrating that a rational design method can be developed for prestressed beams with debonded strands. This research also shows that the currently required multiplier of 2.0 for the development length of debonded strands can be significantly reduced for some cases. Conversely, some dangerous and unsafe designs may be allowed by the current code. More appropriately, the provisions for anchorage of debonded strands may need revision.

In the construction of pretensioned concrete beams, prestressing strands are concentrated in the bottom of the cross section to provide maximum efficiency to resist flexural loads. Because of the concentrated prestressing force, the allowable tensile and/or compressive stresses can be exceeded in the end regions of a simply supported beam.

In the middle regions of a beam, pretensioned stresses are balanced by the dead weight of the member. The traditional method for relieving overstresses in the end regions has been to drape strands upward toward the ends of a pretensioned beam, changing the center of gravity of the

strands and effectively reducing concrete stresses at a beam's ends.

The debonding, or blanketing, of strands is an alternative to draping strands in an effort to control the maximum tensile and compressive stresses in pretensioned concrete highway girders. Debonding, by definition, is the intentional breaking of bond between prestressing strand and concrete. This can be done by applying grease to the strands in the regions requiring debonding; however, the most common practice is to wrap specially made split plastic tubing around the strand to prevent bond of the strand to the concrete. Debonding strands can simplify girder construction; draping of strands is more difficult and more dangerous. Debonding of strands likewise exhibits economic advantages when compared to draping of strands.

Rules governing the use of debonded strands have been established on the basis of limited empirical data[3,4] and engineering judgment. Under current code provisions, the required development length for debonded strand is twice the basic development length, except when zero concrete tension is allowed under service load conditions. These provisions are to prevent beam failure due to the special behavior associated with debonded strand, most notably the possibility of bond failure and subsequent reduction in strength of the member.

A series of static flexural tests were performed on prestressed concrete beams containing debonded pretensioned strands. An analytical model was developed that predicts anchorage failure of debonded strands whenever cracking propagates through the transfer zone of the debonded strands. The test results exhibit excellent correlation with the predicted behavior. From the tests discussed in this study and further development of the models predicting bond failure, design of pretensioned beams with debonded strands should prove to be both economical and safe.

This article is the first of three articles that summarize a comprehensive testing program conducted at the University of Texas to investigate the behavior of pretensioned beams made with debonded strands. This first article reports the test results from beams that were tested with monotonic loads. The second article will report the test results from beams that were subjected to fatigue loads and the third article will draw conclusions from the first and second articles to develop and recommend design guidelines for the use of debonded strands.

CURRENT AASHTO AND ACI CODE REQUIREMENTS

Current code provisions of the American Concrete Institute (ACI)[1] and the American Association of State Highway and Transportation Officials (AASHTO)[2] governing the use of debonded strands are nearly identical. The ACI Code provision is listed as follows:

> ACI Section 12.9.3 – "Where bonding of a strand does not extend to end of member, and design includes tension at service load in precompressed tensile zone, as permitted by Section 18.4.2., development length specified in Section 12.9.1 shall be doubled."

The basic development length is given in ACI Section 12.9.1 as:

$$L_d = \left(f_{ps} - \frac{2}{3} f_{se} \right) d_b \qquad (1)$$

Therefore, based on currently accepted practices and materials, 1.0 $L_d \approx 80$ in. (2.03 m) and 2.0 $L_d \approx 160$ in. (4.1 m) for 0.5 in. (12.7 mm) diameter strands.

This provision requires that debonded strands be bonded for a length equal to twice the required development length for fully bonded strands. An exception is allowed if tension is not allowed in the bottom fiber of the prestressed beam for the service load calculation.

The two times provision is based largely on empirical data obtained from tests conducted by Kaar and Magura (1965).[3] In these tests, beam failures were caused by anchorage failure of the debonded strands if the bonded length was only one times the bonded length given by ACI 12.9.1. On the other hand, when twice the bonded length of ACI 12.9.1 was provided, the beams failed in flexure and strands were fully developed.

In 1979, tests conducted by Rabbat, Kaar, Russell, and Bruce[4] demonstrated that if zero tension were allowed in the concrete at service load, then debonded strands required only one times the development length given by ACI 12.9.1.

Current code provisions reflect the behavioral uncertainty that surrounds the use of debonded strands. Even though the AASHTO Specifications allow debonded strands, many state DOTs do not specify their use because they fear that debonding strands significantly weakens the pretensioned beam. The states of Texas and Oklahoma do not currently allow debonded strands as an alternative to draping strands for I-shaped girders, but they do allow debonded strands in box shapes and other cross sections.

THEORETICAL DEVELOPMENT

The theoretical development predicting the failure behavior of prestressed concrete beams made with debonding strands is simple and straightforward and can be summarized in the following three statements:

1. Cracking through the transfer zone of a pretensioned strand will cause that strand to fail in bond.

2. Debonding strands decreases a beam's resistance to both flexural cracking and web shear cracking in the end regions of a beam.

3. The relationship between bond failure and cracking can be refined and employed to predict the behavior of beams made with debonded strands.

Influence of Cracking on Bond

In early research conducted on the anchorage of pretensioned wires, Janney (1954)[5] predicted that anchorage would fail if a "wave of high bond stress" reaches the transfer zone of the pretensioned wire. He reasoned that because prestress bond developed primarily through the wedging action from Hoyer's effect, bond failure would result if the strand in the transfer zone were required to carry additional tension from external loads.

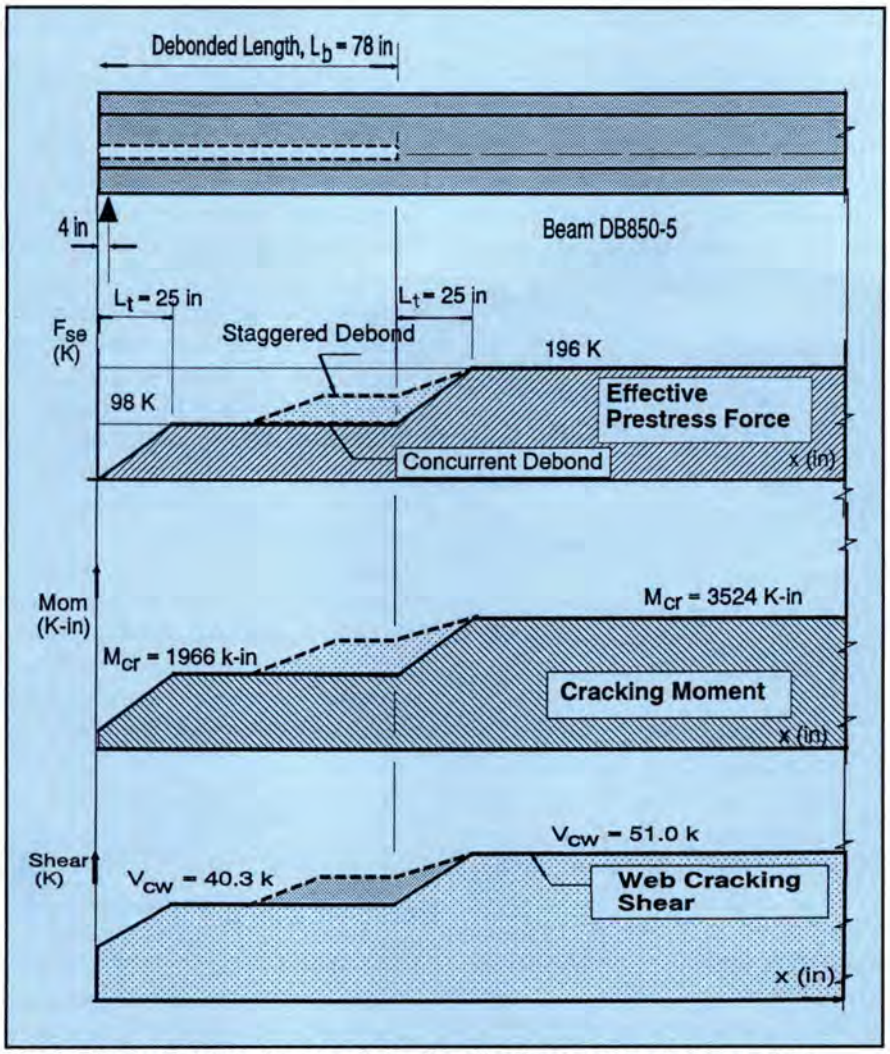

Fig. 1. Effects of debonding strands on the effective prestress force, cracking moment and web cracking shear in end regions of pretensioned beams.

(Hoyer's effect refers to the wedging action that results from Poisson's effect as a pretensioned strand attempts to expand laterally against the concrete in the end regions of a pretensioned member, after the pretensioning force has been released.)

Increases in strand tension cause the strand diameter to diminish; wedging action is destroyed as a result. Flexural tests conducted by Hanson and Kaar (1959)[6] verified that pretensioned anchorage was destroyed when strand tension increased near the transfer zone.

Research conducted at The University of Texas at Austin[7,8] demonstrated that increases in strand tension and subsequent anchorage failures were caused by cracking that propagated through or near the transfer zone of strands. When a crack forms in concrete, tension in the pretensioned steel necessarily increases to resist additional tensile forces required by external loads; tension in the concrete is relieved by the crack. Increases in strand tension, in turn, cause the diameter of the strand to diminish.

Additional strand tension is restrained by bond stresses between the concrete and the steel. Compatibility dictates that local bond slip of the strand must occur over some finite distance immediately adjacent to the crack and the length of bond slip is approximately equal to the length over which the increased tension in the steel is equilibrated by bond stresses. In this manner, cracking causes a "wave of high bond stress" immediately adjacent to a concrete crack.

In pretensioned concrete beams, this mechanism causes anchorage failure whenever a crack forms within or near the transfer zone of a strand. As the concrete cracks, tension in the strand at the crack location must increase. As strand tension increases, strand diameter decreases. In the transfer zone, the strand's lateral expansion that occurred at transfer is negated, and the transfer bond from Hoyer's effect is lost, at least locally.

As the wedging action from Hoyer's effect is eliminated, the strand will slip through the concrete. Upon increased loading, the anchorage of the strands can be expected to fail completely. In this manner, the behavioral model for predicting bond failure of debonded prestressing strands is directly related to a prediction for cracking in the debond/transfer zone of pretensioned concrete girders.

Stated simply, strand anchorage failures are predicted when concrete cracks propagate through or near the transfer zones of pretensioned strands. Furthermore, because cracking in the concrete can be reliably predicted, bond failure of the prestressing strand can also be predicted.

Debonding Strands: Lower Effective Prestress Force

By debonding strands, the effective prestress force is reduced in the end regions of the beams, when compared with beams that contain fully bonded strands. In turn, because of the reduced effective prestress force, debonding of strands also lessens a beam's resistance to flexural cracking and to web shear cracking.

This is demonstrated in Fig. 1, where the effective prestress force is plotted against the length of a beam taken from this test series, Specimen DB850-5. The beam is shown in the top portion of the figure; note that the debonded length is 78 in. (1.98 m). Specimen DB850-5 contained eight strands in total, four of which were debonded. [Authors' note: For each design case, the debonded length, L_b, is arbitrarily selected by the designer. The explanation for the selection of L_b = 78 in. (1.98 m) for this test series is found in the section titled, "Bond Failure Prediction Model."]

Fig. 1 illustrates the increase in the effective prestress force from the end of the beam through the debonded length of the beam and the transfer zone of the

debonded strands, until the prestress force is fully effective. Mirroring the increases in prestress force are similar increases in the beam's resistance to flexural cracking, M_{cr}, and the beam's resistance to web cracking, V_{cw}.

As shown in Fig. 1, the effective prestress force at the end of the beam is zero. Over the first 25 in. (625 mm), the prestress force increases from zero to 98 kips (436 kN), representing the transfer of the four fully bonded strands. Estimating the effective prestress to be 160 ksi (1100 MPa), each 0.5 in. (12.7 mm) diameter strand carries about 24.5 kips (109 kN) of tension and the effective prestress force from the four fully bonded strands is 98 kips (426 kN).

At the point where debonding terminates, 78 in. (1.98 m) from the beam's end, the debonded strands begin to transfer their prestressing force into the concrete, represented by the second transfer zone where the prestressing force increases from 98 to 196 kips (426 to 872 kN). The second transfer zone, as shown, is also 25 in. (635 mm) long, beginning at 78 in. (1.98 m) and extending to 103 in. (2.62 m) from the end of the beam.

The transfer length assumed for these models is 25 in. (635 mm), an approximate average of the measured transfer lengths from earlier testing.[9] For many of the AASHTO-type beams, the measured transfer length was actually less than 25 in. (635 mm), but for other beams it was much larger than 25 in. (635 mm). It should be noted that longer transfer lengths will adversely affect a beam's behavior because the region of reduced prestress is extended towards the middle of the beam.

Staggered Debonding vs. Concurrent Debonding

In the figure, dashed lines are shown labeled "Staggered Debond." The solid line is denoted as "Concurrent Debond." In beams with staggered debonding, the termination points of various strands are "staggered," meaning that the debonded length varies from strand to strand. In concurrently debonded beams, the termination point is the same for all of the debonded strands.

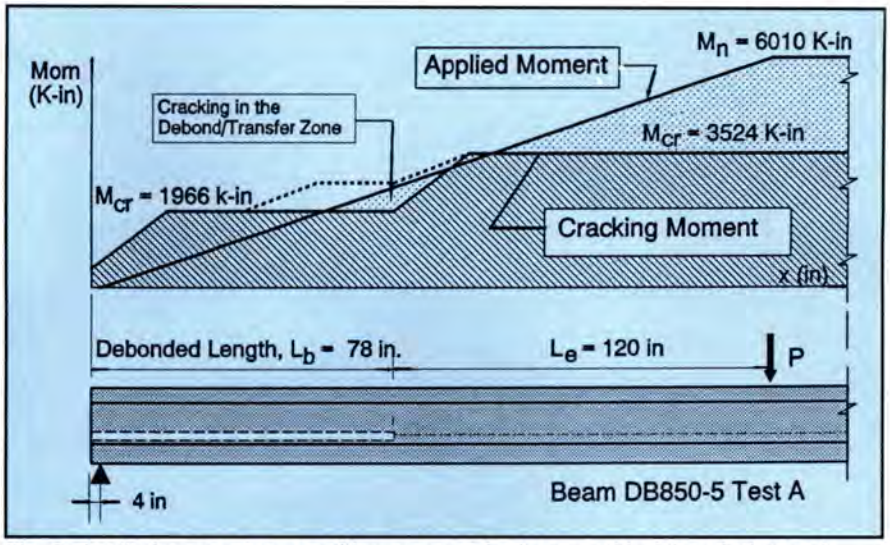

Fig. 2. Applied moment vs. cracking moment for beams with debonded strands.

For example, Specimen DB850-5 contained concurrently debonded strands where all four of the debonded strands were debonded the same length, L_b = 78 in. (1.98 m). On the other hand, Specimen DB850-4 contained a staggered debonding pattern where two of the four debonded strands were debonded for 39 in. (0.99 m) and the other two debonded strands had debonding that terminated at 78 in. (1.98 m).

The debond length, L_b, was 78 in. (1.98 m) for both specimens; however, the behavior of concurrently debonded specimens was quite different from specimens with staggered debonding. Staggering the debonding has the effect of gradually increasing the effective prestress force through the debonded regions, thus improving the beam's resistance to cracking.

For the purposes of these tests, the concurrently debonded specimens help dramatize the results. Also, they illustrate some of the special problems inherent with concurrently debonded specimens. Staggered debonding is recommended based on the tests performed in this research.

Debonding Strands: Effects on Flexural Cracking

The impact of debonding is shown in Fig. 2 where applied moment is compared to the beam's cracking moment, M_{cr}. Here, M_{cr} is defined as the applied moment that causes flexural cracking in the bottom tension fiber of the cross section; it is calculated based on a bottom fiber tension equal to the modulus of rupture, $7.5\sqrt{f'_c}$. M_{cr} is a property of the beam and is dependent on the cross section properties and the effective prestress force.

As shown in the figure, the cracking moment increases as the effective prestress force increases. Again, the difference between the "concurrently debonded" specimens and the "staggered debonded" specimens is displayed in the figure.

At the end of the beam, the effective prestress force is zero and the cracking moment is given by the section modulus multiplied by the modulus of rupture: $M_{cr} = S_b \times 7.5\sqrt{f'_c}$. Progressing from the end of the beam, M_{cr} increases due to the corresponding increase in the effective prestress force. Outside the initial transfer zone, M_{cr} remains approximately constant until the debonded strands become bonded and additional prestressing force is transferred to the concrete. At the end of the second transfer zone, the beam exhibits the fully effective prestress force from all its strands. Not until this point does the beam's resistance to flexural cracking reach its full potential.

As external load is applied to the beam, the applied moment increases linearly from the support to the load point (where dead load moment is neglected). As the load increases, the moment also increases; flexural cracking can be expected wherever the applied moment exceeds the cracking moment. From Fig. 2, flexural crack-

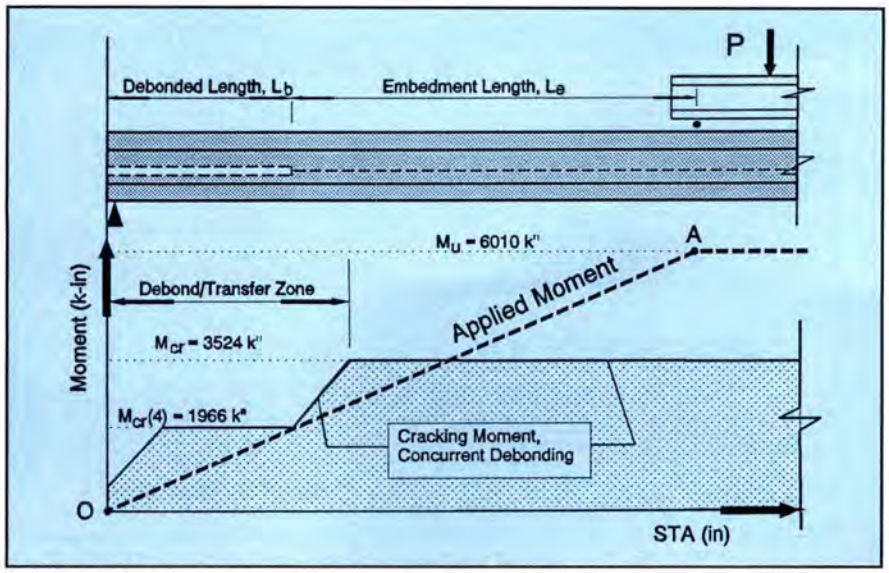

Fig. 3. Applied moment vs. cracking moment for beams with concurrent debonding patterns.

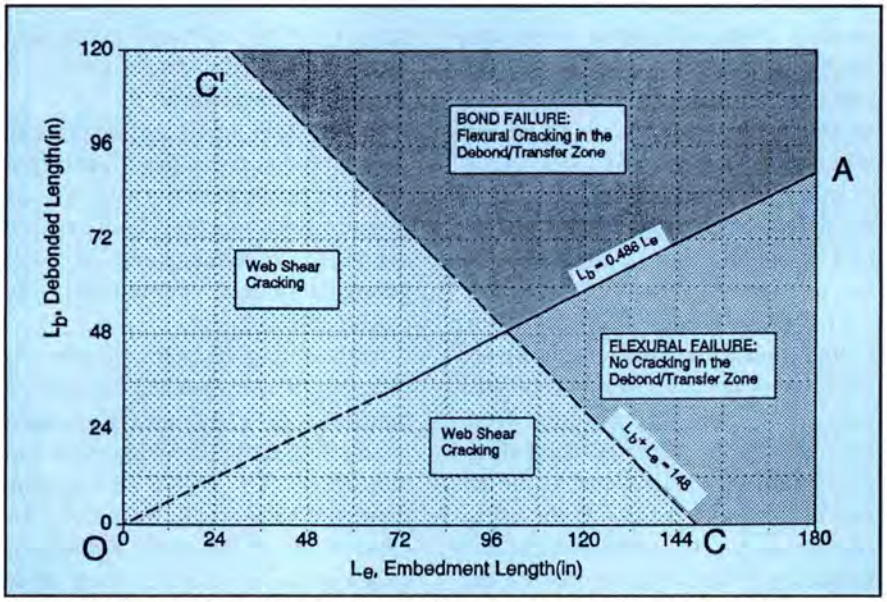

Fig. 4. Prediction of cracking and bond failure for beams with concurrent debonding patterns (DB850 Test Series).

ing will occur primarily in the regions of the largest applied moment, near the load point. As load increases, the region of flexural cracking expands with the region where the applied moment exceeds M_{cr}.

In a beam with fully bonded strands, only one region of flexural cracking would be expected. However, in beams with debonded strands, flexural cracking can occur in the debond/transfer zone, toward the end regions of the beam. In this example, the cracking moment for the debond/transfer zone is exceeded before the nominal flexural capacity of the section is achieved, as shown in Fig. 2.

According to the behavioral model outlined above, cracking in the transfer zone of the debonded strand will cause the debonded strands to slip, creating the physical conditions that make bond failure probable. In fact, the flexural test on Specimen DB850-5A resulted in bond failure of the debonded strands, as a direct result of cracking in the debond/transfer zone. Fig. 2 also illustrates that staggered debonding precludes cracking in the debond/transfer zone.

Bond Failure Prediction Model

The preceding sections show that debonding some pretensioned strands has the effect of reducing the effective prestress force in the end regions of a beam, when compared to beams made with fully bonded strands. A beam's resistance to flexural and shear cracking is also reduced. Furthermore, cracking in the transfer zone of a strand will cause that strand to slip or fail in bond. It follows that if these principles are applied to design, the probable bond failures of debonded strands can be predicted. Likewise, debonding patterns could be designed so that bond failures of the debonded strands would not occur.

In Fig. 3, Line OA represents the applied moment for the embedment length that divides bond failure from flexural failure. At Point O, the applied moment is zero. (Point O is located approximately at the end of the beam.) Point A designates the location where load is applied (and consequently, the point of maximum moment). In this illustration, Point A is selected so that Line OA passes through a third point, within the debond/transfer zone where the applied moment intersects the beam's cracking moment.

If the embedment length, L_e, were increased, the line of applied moment would move to the right and flexural cracking would occur only in regions outside the debond/transfer zone. Strand anchorage would be undisturbed by flexural cracking and, consequently, the beam could be expected to achieve its flexural capacity and bond failures would not occur.

However, if the embedment length were decreased, the line of applied moment would move to the left and the beam's cracking moment would be exceeded in the transfer zone of the debonded strands (debond/transfer zone). The shorter embedment length would be expected to produce a strand bond failure before the flexural capacity of the beam was reached.

In this model, Line OA forms a boundary line between flexural failures and bond failures. From similar triangles, Line OA is defined by the relationship:

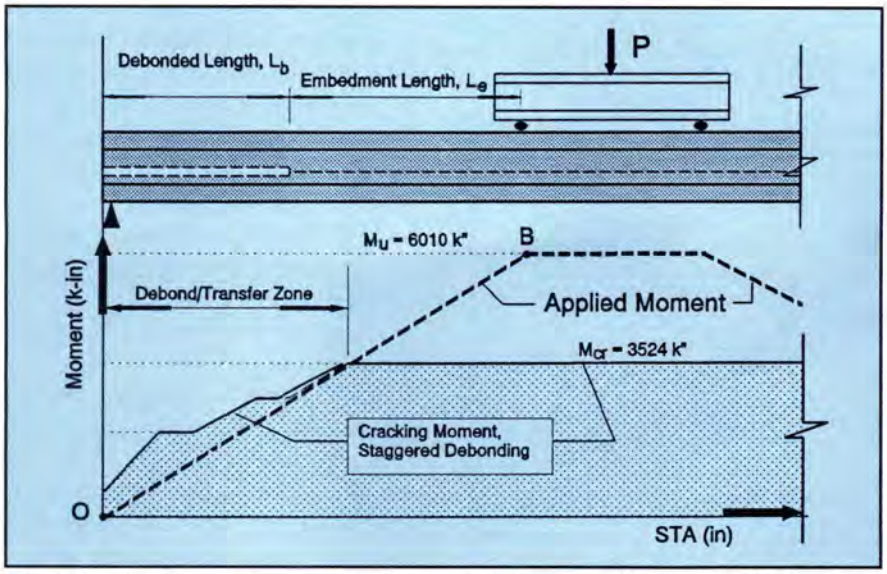

Fig. 5. Applied moment vs. cracking moment for beams with staggered debonding.

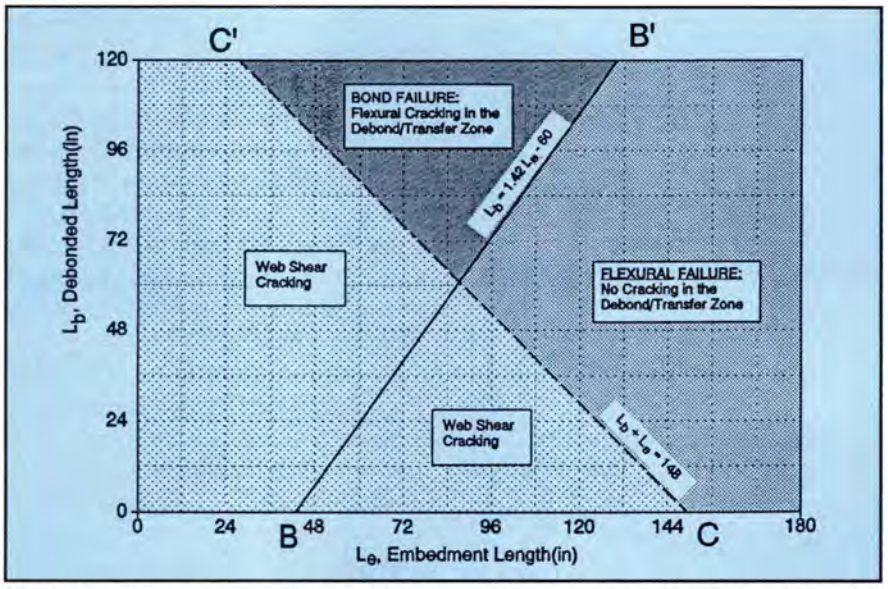

Fig. 6. Prediction of cracking and bond failure for beams with staggered debonding patterns (DB850 Test Series).

$$\frac{M_{cr4}}{L_b} = \frac{M_n}{L_b + L_e} \qquad (2)$$

For a specific design case, the appropriate values can be substituted into the equation. For the beams of this test series, M_n = 6010 kip-in. (679 N-m) and M_{cr4} = 1966 kip-in. (222 N-m). An equation relating embedment length to debonded length can then be established:

$$L_b = 0.486\,L_e \qquad (2a)$$

This equation is plotted on the graph in Fig. 4. The plot predicts the mode of failure for combinations of embedment length and debonded length. Line OA also appears in Fig. 4 as the boundary line between flexural failures and bond failures. The shorter embedment lengths to the left and above Line OA make bond failures predicted. Likewise, below and to the right of Line OA, flexural failures are predicted.

A relationship can also be established that predicts the occurrence of web shear cracking. Web shear cracking was shown to cause anchorage failures in many pretensioned I-shaped beams,[7,8,10,11] though not all.[12] The relationship predicting the occurrence of web shear cracking is given by:

$$L_b + L_e = \frac{M_n}{V_{cw4}} \qquad (3)$$

For the test series beams, the value for V_{cw4} is 40.7 kips (181 kN), calculated at a distance from the support equal to the height of the beam. By substituting the values for M_n and V_{cw4}, the equation above reduces to:

$$L_b + L_e = 148 \qquad (3a)$$

This line is shown in Fig. 4 as the Line CC′.

For beams with strands in a staggered debonding pattern, a similar relationship can be established separating bond failure from flexural failure. In Fig. 5, this condition is given by Line OB. Line OB is defined by the applied moment that would cause flexural cracking to occur at the extreme end of the debond/transfer zone.

If the load point were moved left and strand embedment were shortened, then cracking would occur in the debond/transfer zone, and bond failure would be predicted. Likewise, if the load point were moved to the right and strand embedment were lengthened, then flexural cracking would occur outside the debond/transfer zone; strand anchorage would be unaffected and flexural failure is likely.

From Fig. 5, it should be noted that varying combinations of the number of strands that are debonded with varying debonded lengths could produce even more gradual increases in effective prestress force. Therefore, the point of first cracking for a beam with staggered debonding will usually occur at the end of the debond/transfer zone.

The mathematical relationship for Line OB is given by similar triangles:

$$\frac{M_{cr}}{L_b + L_t} = \frac{M_n}{L_b + L_e} \qquad (4)$$

Substituting calculated values for M_{cr} = 3524 kip-in. (398 N-m), M_n = 6010 kip-in. (679 N-m) and L_t = 25 in. (635 mm), an equation relating L_b and L_e is given:

$$L_b = 1.42\,L_e - 61 \text{ in.} \qquad (4a)$$

This relationship is illustrated by the Line BB′ in Fig. 6. Areas to the left of the line, with shorter embedment

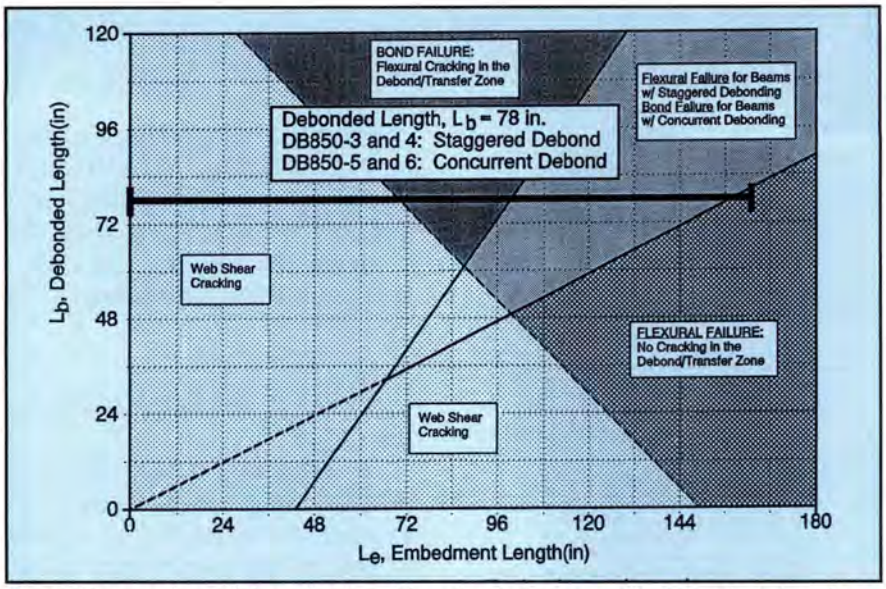

Fig. 7. Range of possible embedment lengths for beams with debonded strands.

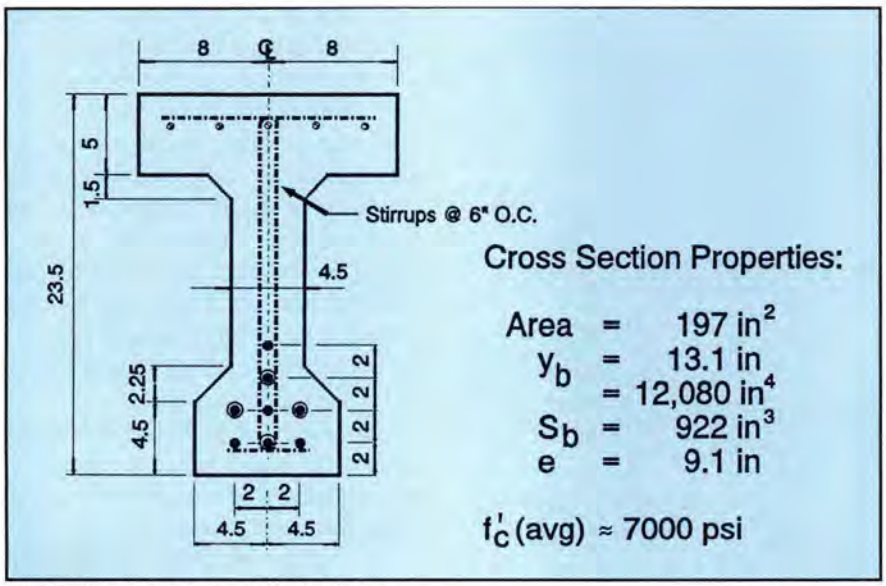

Fig. 8. Cross section of DB850 beams.

lengths, result in bond failures while regions to the right of Line BB′ result in flexural failures.

Two important facts are illuminated by the plots in Figs. 4 and 6. First, the embedment length necessary to prevent bond failures is dependent on the length of debonding. Second, longer debonded lengths require greater embedment lengths to ensure strand anchorage. Therefore, it is incumbent upon the designer to maintain the debonded lengths of strand at their shortest possible distance. Guidance for the design of debonded lengths is found in Ref. 13.

Fig. 7 combines the plots from Figs. 4 and 6 to illustrate some important concepts. The regions of the plot clearly indicate the predicted outcome from tests for a wide range of possible embedment lengths, debonded lengths and debonding patterns. Of course, the values and predictions obtained from Fig. 7 are specific to the cross section, the number of strands, and the number of debonded strands. However, results from this testing program can be translated into more generalized design guidelines, especially when their agreement with the predicted behavior is considered.

The range of possible test variables with the chosen debonded length of 78 in. (1.98 m) is shown in Fig. 7. In design, the need for debonding and the lengths of debonding are dictated by the allowable stress requirements. For these tests, the debonded length of 78 in. (1.98 m) was selected because this length offered the greatest range of possible outcomes.

With a debonded length of 78 in. (1.98 m), the embedment lengths could be chosen so that varying test results, bond failures, or flexural failures for either concurrent or staggered debonding patterns could be obtained. The debonded length of 78 in. (1.98 m) also offered the opportunity to test embedment lengths between 1.0 and 2.0 times the basic development length given in ACI 12.9 and by AASHTO Eq. (9-32) [1.0 $L_d \approx 80$ in. (2.03 m)].

Fig. 7 also clearly illustrates the embedment length that is required to develop flexural failures in the test series. From the figure, an embedment length of approximately 100 in. (2.5 m) is required to develop adequate tension in debonded strands from a staggered debonding pattern. An embedment length of approximately 160 in. (4.0 m) is required to develop debonded strands that are part of a concurrent debonding pattern.

Finally, the figure helps to illustrate the predicted differences between staggered and concurrent debonding patterns. It clearly shows that debonded strands in a staggered debonding pattern should require less strand embedment to develop flexural failures than debonding patterns that are concurrent. From this model, beams with staggered debonding patterns should demonstrate superior bond performance compared to beams with concurrent debonding patterns.

TESTING PROGRAM

Six flexural tests were performed on four beam specimens. Each beam contained eight 0.5 in. (12.7 mm) diameter strands; four strands in each beam were debonded and four strands were fully bonded to the ends of the beam. The beams possessed nearly identical cross sections, as illustrated in Fig. 8. The properties for the gross cross section are given in the figure. Beam Specimen DB850-3 was only 23 in.

Table 1. Variables by test specimen for DB850 beams.

Test	Beam length L (in.)	Debonded length L_b (in.)	Embedment length, L_e (in.)	Type of debonding*
DB850-3A	480	78	80	S
DB850-3B	480	78	108	S
DB850-4A	480	78	120	S
DB850-4B	480	78	100	S
DB850-5A	480	78	120	C
DB850-6A	480	78	150	C

Note: 1 in. = 0.0254 m.
* "S" denotes staggered debonding; "C" denotes concurrent debonding.

Table 2. Concrete strengths of beams with debonded strands (in psi).

Beam	Release strength (psi)	Strength at flexural test	
		Moist cure	Field cure
DB850-3	5080	6610	6830
DB850-4	5060	7370	6860
DB850-5	5580	7460	–
DB850-6	5150	6940	7300

Note: 1 psi = 0.006895 MPa.

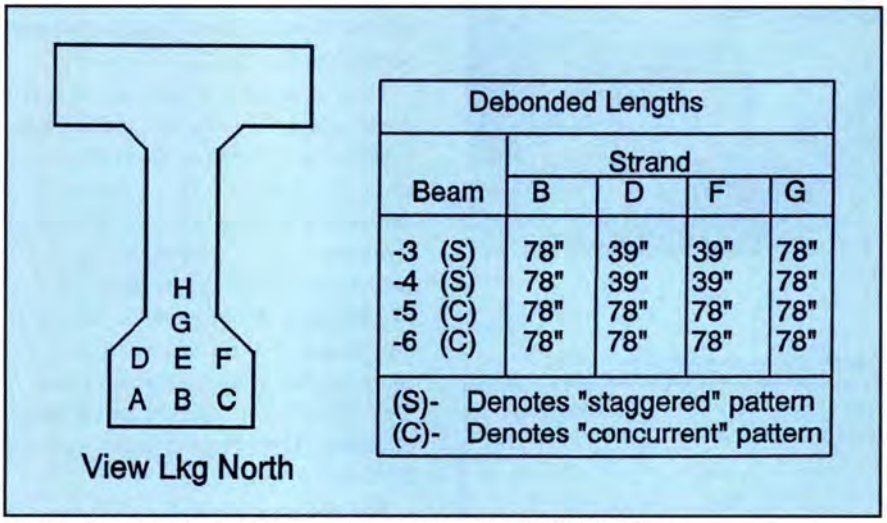

Fig. 9. Strand pattern and debonding schedule for DB850 beams.

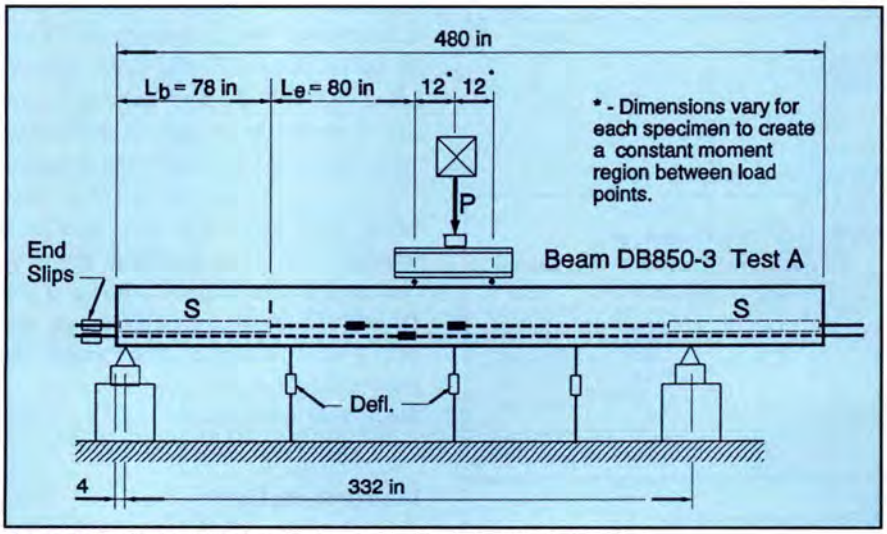

Fig. 10. Typical test setup for beams with debonded strands.

(584 mm) deep, so its properties varied slightly from the other specimens.

Vertical shear reinforcement, consisting of pairs of #3 bars, was spaced at 6 in. (152 mm) for all specimens. No variation was made in shear reinforcement along the length. No special confining steel or anchorage details were provided on any strands. Each beam was 40 ft (12.1 m) in length.

Variables

The variables tested for the debonded beams included: type of debonding cutoff [staggered (S) or concurrent (C)], and embedment length, L_e.

Table 1 gives the embedment length, the debonded length, and the type of debonding for each specimen. In Specimens DB850-3 and DB850-4, cutoff points for debonding strands were staggered. Specimens DB850-5 and DB850-6 contained concurrently debonded strand patterns.

Fabrication of Test Specimens

Fabrication of the beams followed the basic procedure outlined as follows: stress strands to 75 percent of f_{pu}, place the mild steel reinforcement, place the debonding material, place the formwork, cast the concrete, cure the concrete in place (approximately two days), and release the pretensioning (approximately 48 hours after casting).

The debonding material consisted of white plastic tubing, made from semi-rigid plastic. The plastic tubing was placed on the strand where debonding was required. The tubing's natural curl snapped it to the strand, providing a reasonably tight fit. The debonding material was sealed with tape at each end, but the seam at the longitudinal split fit tightly and was not taped.

The strands are labeled in Fig. 9 by letters of the alphabet, A through H, to simplify record keeping. The debonding schedule is also shown in the figure. Note that the debonded strands B and G are contained within the core of shear reinforcement.

Materials

Pretensioning strand was donated by Florida Wire and Cable Company (FWCC). The strand surface was "mill condition" as furnished, having been free from exposure to weathering environments. Strand was stored in the laboratory where it was kept reasonably free of rust. Strand from the same

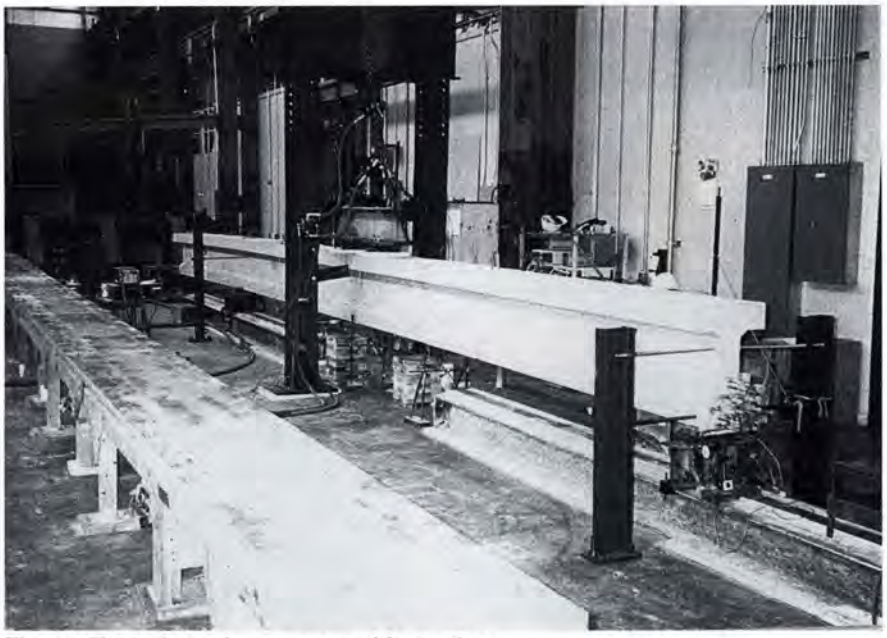

Fig. 11. Typical specimen prepared for testing.

Table 3. Summary of flexural tests on beams with debonded strands.

Test	Debonded length L_b (in.)*	Embedment length, L_e (in.)	Percent L_d†	Failure mode
DB850-3A	78(S)	80	1.00	Bond
DB850-3B	78(S)	108	1.35	Flexure
DB850-4A	78(S)	120	1.50	Flexure
DB850-4B	78(S)	100	1.25	Flexure with slip
DB850-5A	78(C)	120	1.50	Bond
DB850-6A	78(C)	150	1.875	Flexure/Bond

Note: 1 in. = 0.0254 m.

* "S" denotes staggered debonding; "C" denotes concurrent debonding.

† $L_d \approx 80$ in. (2.03 m); $f_{ps} = 260$ and $f_{se} = 150$ ksi (1793 and 1034 MPa).

Table 4. Applied load at failure tests on beams with debonded strands.

Beam	L_b (in.)	Ultimate load			Concrete strain at ultimate (in./in. x 10^{-6})	Failure mode
		P_u (kips)	$M_{u,test}$ (kip-in.)	$\frac{M_{u,test}^*}{M_n}$		
DB850-3A	78(S)	69.58	5358	0.91	2844	Bond
DB850-3B	78(S)	69.32	5615	0.96	2896	Flexure
DB850-4A	78(S)	70.33	6038	1.00	2808	Flexure
DB850-4B	78(S)	75.39	6029	1.00	2704	Flexure
DB850-5A	78(C)	81.16	6017	1.00	2136	Bond
DB850-6A	78(C)	52.24	5851	0.97	2876	Flexure/Bond

Note: 1 in. = 0.0254 m; 1 kip = 4.448 kN; 1 kip-in. = 0.113 kN-m.

* $M_n = 6010$ kip-in. for Beams DB850-1, 2, 4, 5 and 6; $M_n = 5870$ kip-in. for Beam DB850-3.

spool was used for all tests. The strand's ultimate strength was specified at 270 ksi (1860 MPa) and low relaxation strand was used for these tests. The strand's ultimate strength was 283 ksi (1950 MPa), as reported by the manufacturer.

The concrete strengths were designed to be 4500 psi (31 MPa) at release and 6000 psi (41 MPa) for 28-day strength. Concrete strengths for the DB850 series beams are given in Table 2.

Testing Apparatus

A typical test setup is shown schematically in Fig. 10. The dimensions illustrate the setup for Test DB850-3A; debonding for this beam was "staggered." In this debonding pattern, debonding covered two strands for a length of 78 in. (1.98 m) from the end of the beam while the other two debonded strands were staggered, with debonding terminated at 39 in. (0.99 m). The staggered debonding pattern is denoted with an "S" above the representation for debonded strands. For this test, the embedment length was set at 80 in. (2.03 m) to correspond to the 1.0 times the required development length given by AASHTO Eq. (9-32).

The embedment length, L_e, and span were varied for each test and were defined as the distance from the maximum moment to the point where debonding was terminated. A constant moment region was maintained between the load points in all of the tests by matching the proportions of the dimensions of the load on top of the spreader beam with the proportions of the overall beam support and load application. The spreader beam spanned 24 in. (610 mm).

The photograph in Fig. 11 shows a test specimen in the testing apparatus, located on the reaction floor at the Phil M. Ferguson Structural Engineering Laboratory, The University of Texas at Austin, Austin, Texas. Load was applied through the hydraulic actuator and spreader beam shown. End slips were measured from the linear potentiometers pictured at the end of the test beam. Each beam was supported by a pinned connection, shown at the near end, and a roller support, shown at the far end. In the background appear the heavy steel buttresses that formed the prestressing bed for the fabrication of the pretensioned beams.

Instrumentation

Instrumentation measured the applied load, beam deflections, and strand end slips. These data were measured electronically and stored by the data acquisition system. Load was measured from an electronic load cell at the point of load application. Deflection and end slips were measured by linear potentiometers. All of the electronic instruments were calibrated prior to testing. End slip measurements are believed to be accurate to ± 0.001 in. (0.025 mm),

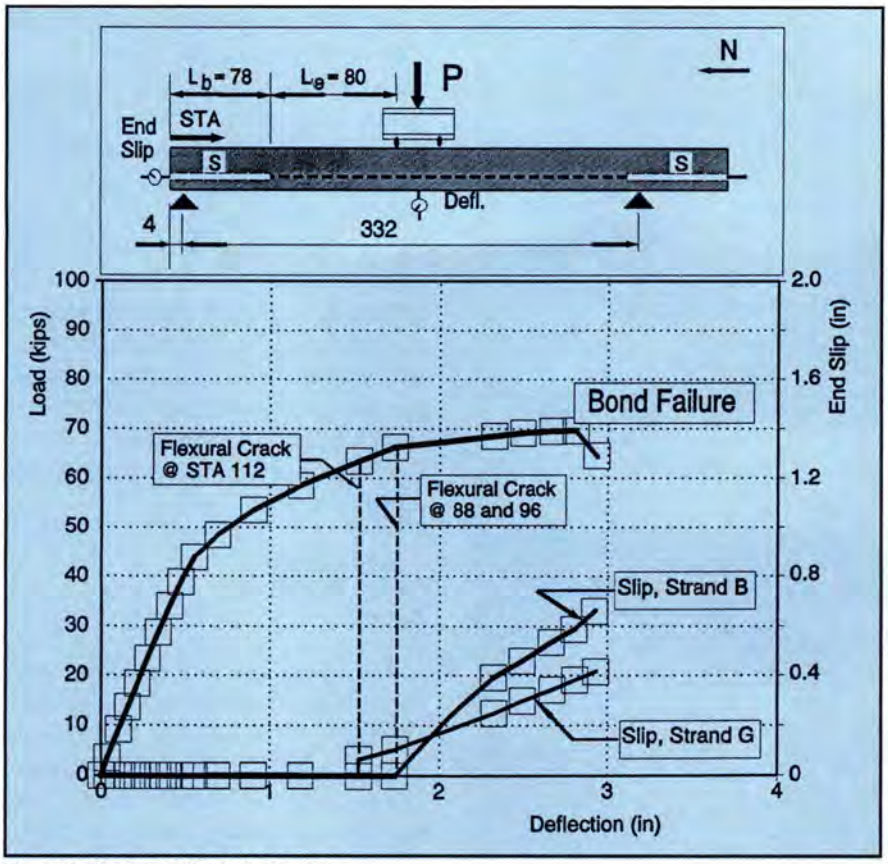

Fig. 12. Beam DB850-3, Test A.

thus, even very small strand slips were detected. Top fiber concrete strains were measured in the constant moment region for each test using mechanical strain gauges.

End slips were measured on seven of the eight strands, including the four debonded strands, B, D, F and G. Strand E was the only strand not monitored for end slip due to geometric constraints at the ends of the beams.

Test Procedure

The beams were loaded statically until failure. Load was increased at regular increments by increasing the hydraulic pressure supplied to the ram. Data were taken and measurements were recorded at each load increment in approximately 2.0 to 5.0 kip (8.9 to 22.2 kN) increments until cracking. Cracking loads and crack locations were noted and recorded. After cracking, the load was increased in smaller increments.

Any special behavior was noted and crack patterns were marked with a broad ink marker on the specimen. Significant end slips were noted and recorded. Failure was defined by the beam's inability to sustain load through increasing deformations. Flexural failures resulted when the top flange of the beam failed in compression. Anchorage failures resulted in general slip of the strand relative to the concrete and a sudden loss of capacity.

Beams DB850-3 and DB850-4 were tested twice, once at each end. The first test on a specimen is designated Test A while the second test is designated Test B. Two tests were possible on these beams because Test A did not damage the anchorage zone at the opposite end of the beams. In the cases of Beams DB850-5 and DB850-6, the longer development length requirements precluded an effective second test.

TEST RESULTS

In reviewing results from the tests, the mode of failure is the primary indicator of anchorage performance. Two types of failures were observed in this series of tests, flexural failure and bond, or anchorage, failure. Flexural failures were evidenced by crushing of the concrete after yielding of the strand and were characterized by the ability of the beams to resist the nominal flexural moment, combined with the ability to sustain that load through large deformations. Therefore, two criteria, capacity and ductility, were required to classify a failure as a flexural failure. By meeting the criteria of capacity and ductility, a beam demonstrates a predictable load capacity with reasonable warning before collapse, and thereby provides a safe and reliable structure.

Anchorage failures, also called bond failures, were characterized by general slip of one or more strands through the concrete, as measured from the end of the beam. Additionally, anchorage failures typically were unable to develop the nominal flexural capacity of the beam. Interestingly, anchorage failures on beams with debonded strands are ductile failures because the strands that are fully bonded are capable of developing the strand tension required to yield the strand.

Test results are shown in Tables 3 and 4. Table 3 summarizes the failure mode for each test and compares the embedment length, L_e, to the required development length, L_d. The embedment length is measured from the debond termination point to the point of maximum moment. L_d is calculated using AASHTO Eq. (9-32) (ACI Section 12.9).

Table 4 compares the maximum moment at failure, M_u, with the calculated nominal capacity. In cases of flexural failure, the tested maximum moment nearly equals or exceeds the calculated flexural capacity. If a beam's ultimate capacity at failure does not approach the nominal flexural capacity of the section and significant strand slips have occurred, then anchorage failure of the strands is indicated. Note that even in extreme cases of obvious bond failures, the section still achieves a very large percentage of the nominal capacity.

Beam DB850-3, Test A

Beam DB850-3 contained four debonded strands in a staggered cutoff pattern. Strands B and G were debonded to the full debonded length of 78 in. (1.98 m); Strands D and F were debonded to only 39 in. (0.99 m). Fig. 12 plots the load vs. deflection for

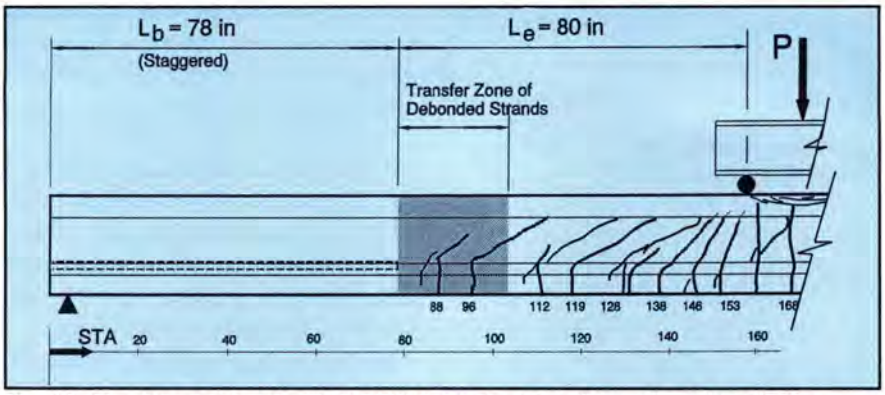

Fig. 13. Cracking pattern for Test DB850-3A depicting flexural cracking in the transfer zone of debonded strands.

Fig. 14. Cracking pattern for Test DB850-3A — Cracking in the debond/transfer zone and bond failure of debonded strands.

Test DB850-3A, and demonstrates a typical bond failure for beams with debonded strands. Note that the embedment length, L_e = 80 in. (2 m), approximates 1.0 times the basic development length given by AASHTO Eq. (9-32) and ACI 12.9. Fig. 12 also shows the test dimensions.

The first flexural crack occurred at a load of 43.8 kips (195 kN), corresponding to a flexural cracking moment of 3376 kip-in. (372 N-m) — within 5 percent of the cracking moment predicted by elastic analysis and a modulus of rupture of $7.5\sqrt{f'_c}$. As load increased, the number of cracks also increased and flexural cracking progressed from the load point towards the beam's support.

At a total load of approximately 64 kips (285 kN), formation of the crack at Station 112 [112 in. (2.84 m) from the beam's end] coincided with the initial slip on Strand G. Station 112 is just outside of the debond/transfer zone (the transfer lengths of these prestressing strands are imprecisely quantified). At a total load of 66.3 kips (295 kN), flexural cracks formed at Stations 88 and 96 and general bond slip ensued.

The cracking patterns for Test DB850-3A are illustrated in Fig. 13 and a photograph of the beam is shown in Fig. 14. Note the cracks at Stations 88 and 96. Upon formation of these cracks, Strands B and G were observed to slip. These two strands were the only strands affected by the cracking. The other two debonded strands, Strands D and F, were unaffected because their transfer zone began at Station 39 and theoretically ended at Station 64. None of the other strands slipped and the beam continued to resist load.

Despite the appearance of flexural failure, this beam failed due to loss of anchorage for the debonded strand. Its failure is classified as a bond failure because the failure load was significantly less than its nominal flexural capacity. Test DB850-3A failed at a load of 69.6 kips (309 kN), resulting in a maximum applied moment of 5358 kip-in. (591 N-m), only 91 percent of the calculated nominal capacity. Note that the dead load moment for this test was 116 kip-in. (13 N-m) at the center of the span and its inclusion does not significantly affect the result.

Beam DB850-4, Test A

Beam DB850-4 also contained four debonded strands with a staggered cutoff pattern. However, the embedment length for Test DB850-4A was 120 in. (3.1 m) compared to only 80 in. (2 m) for Test DB850-3A. Test A on Beam DB850-4 characterizes a typical flexural failure, failing at a load nearly equal to its nominal capacity while sustaining large deformations beyond yielding of the strand.

In Test DB850-4A, the first flexural cracks occurred at a load of 41.7 kips (186 kN), corresponding to an applied moment of 3580 kip-in. (395 N-m), only 1.5 percent greater than the calculated cracking load. Loading was continued until flexural failure occurred at 70.3 kips (313 kN). Flexural failure was evidenced by crushing of the concrete after yielding of the strand. Load is plotted vs. deflection and end slips in Fig. 15. The maximum applied moment was 6035 kip-in. (666 N-m), or 100.4 percent of the calculated nominal capacity. Concrete strains exceeded 2800 microstrains [2800 x 10^{-6} in./in. (mm/mm)] at crushing. Total midspan deflection exceeded 4.5 in. (114 mm).

Flexural cracking did not extend into the transfer zone of the debonded strands and no significant end slips were observed. The nearest flexural crack from the support was located at Station 118. The photograph in Fig. 16 illustrates the flexural cracking patterns observed in this and other flexural failures.

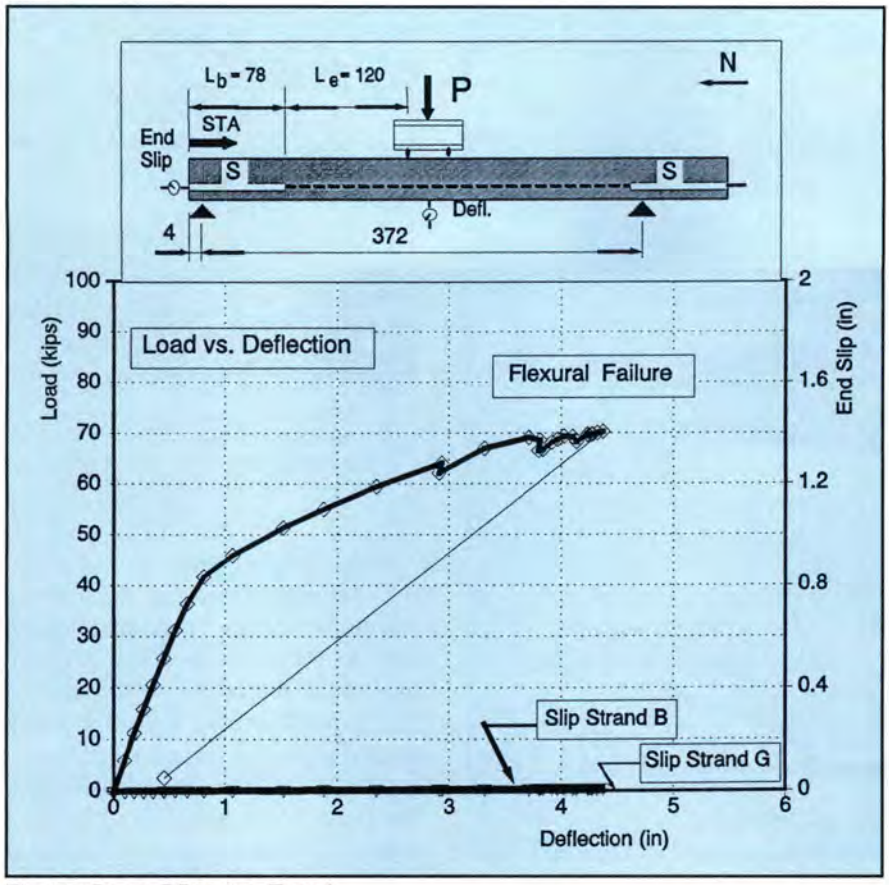

Fig. 15. Beam DB850-4, Test A.

Fig. 16. Cracking pattern for Test DB850-4A — Typical for flexural failures.

Tests DB850-3B and DB850-4B

Tests DB850-3B and DB850-4B also used debonded lengths of 78 in. (1.98 m) with staggered debonding. Load vs. deflections plots and end slips for Tests DB850-3B and DB850-4B are shown in Figs. 17 and 18, respectively. Test DB850-3B had an embedment length of 108 in. (2.74 m) and Test DB850-4B had an embedment length of 100 in. (2.54 m). Both of these tests exhibited flexural behavior by achieving the nominal flexural capacity while sustaining load resistance through large deformations.

Although considered flexural failures, Strands B and G did experience some slipping. For Test DB850-4B at failure, the total slip for Strand B was 0.28 in. (7.1 mm) and the total slip for Strand G was 0.12 in. (3.0 mm). For this test, strand slips were initiated by flexural cracking at Stations 108 [at a load of 71.4 kips (328 kN)] and at Station 95 [at a load of 75.1 kips (334 kN)]. The beam failed in flexure at a total load of 75.4 kips (335 kN). Despite the cracking and end slips, the beam's overall behavior and failure mode were not affected because these cracks did not form until the ultimate load was nearly achieved.

Beam DB850-5, Test A

Beam DB850-5 contained four debonded strands in a concurrent cutoff pattern, meaning that all debonding terminated 78 in. (1.98 m) from the beam's end. Test DB850-5A had an embedment length, L_e, of 120 in. (3.1 m). As noted above, Test DB850-4A, at an embedment length of 120 in. (3.1 m), proved adequate for development of the debonded strands. However, Beam DB850-5 had concurrent debonding compared with the staggered debonding of Beam DB850-4.

The beam in Test DB850-5A failed due to the bond failure of debonded strands. The plot of load vs. deflection and end slip is shown in Fig. 19. Flexural cracking was initiated at a load of 51.8 kips (230.4 kN), about 1 percent larger than the calculated cracking moment. As load increased, cracking extended towards the debond/transfer zone. At a load of 77.8 kips (346.1 kN), flexural cracks propagated through the debond transfer zone. Initial strand slips were caused by the crack that formed at Station 80. This crack was followed by another crack at Station 92. At failure, strand slips measured approximately 0.9 in. (23 mm) on Strand B and 0.8 in. (20 mm) on Strand G. Strands D and F also experienced slips in excess of 0.5 in. (12.7 mm), but are not shown in the figure.

Beam DB850-6, Test A

Beam DB850-6 was fabricated with the identical debonding pattern of Beam DB850-5. Test DB850-6A failed in much the same manner as Test DB850-5A; however, its embedment length of 150 in. (3.8 m) was long enough to induce a hybrid failure of flexural and bond failure. Load vs. deflections and end slips are shown in Fig. 20. This test is classified primarily as a flexural failure because, at failure, the end slips remain relatively small, on the order of 0.01 to 0.02 in. (0.254 to 0.508 mm).

First flexural cracking occurred at 31.3 kips (139 kN), approximately equal to the predicted cracking load.

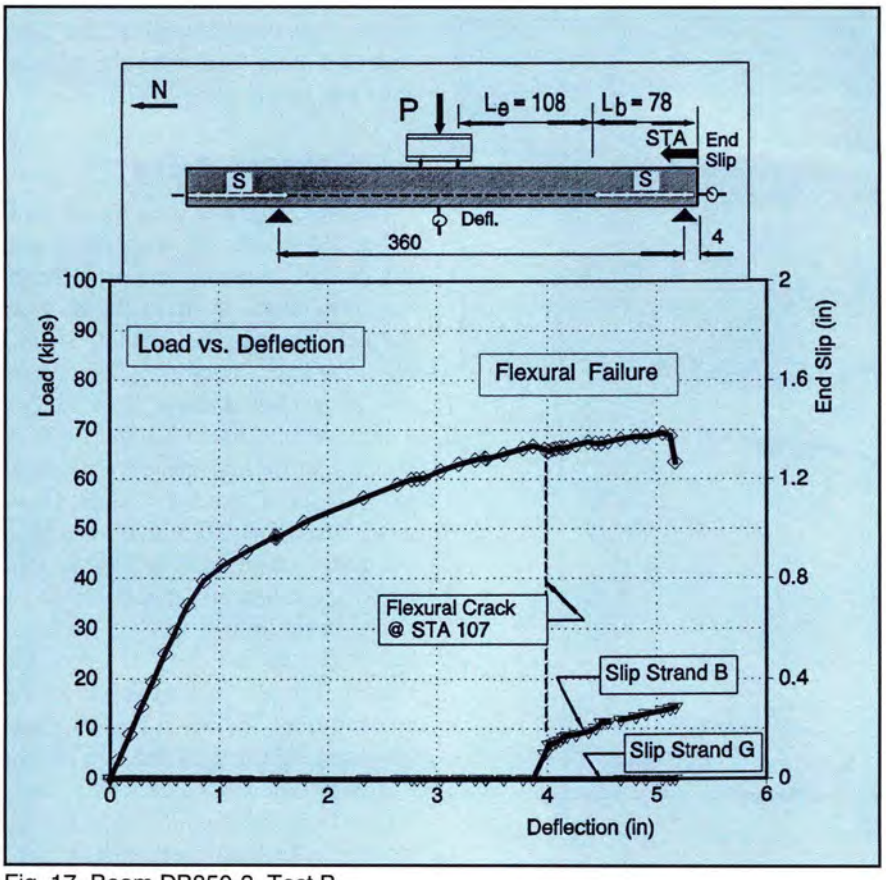

Fig. 17. Beam DB850-3, Test B.

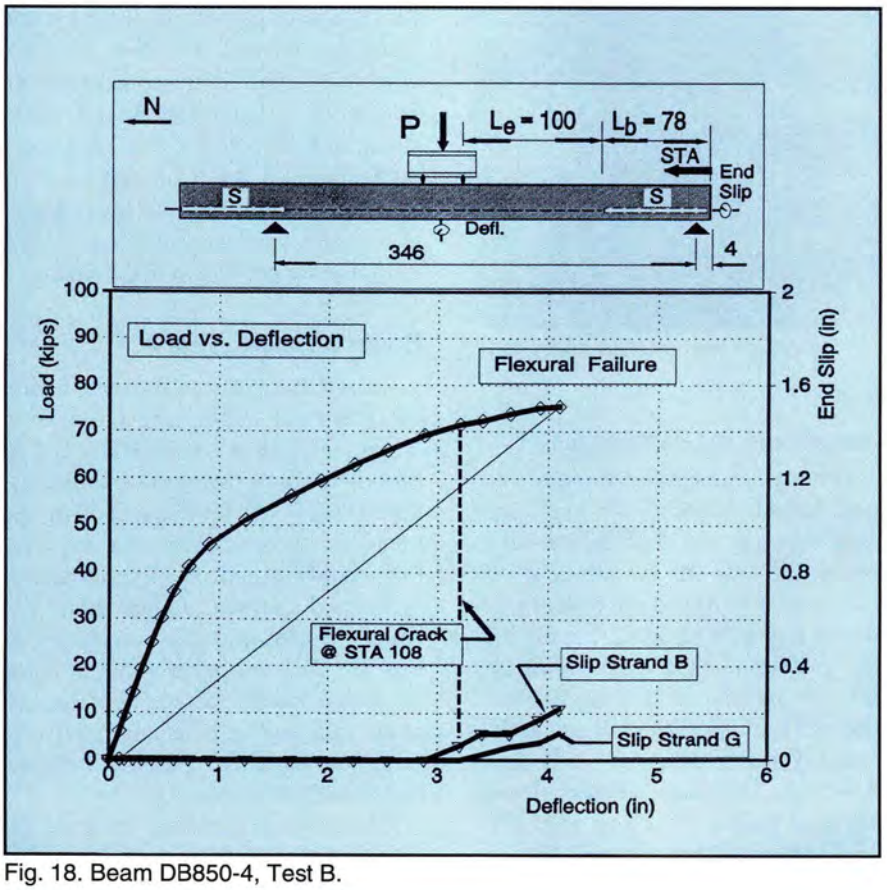

Fig. 18. Beam DB850-4, Test B.

Table 5. First cracking loads and moments tests on beams with debonded strands.

Beam	First cracking		
	P_{cr} (kips)	Moment (kip-in.)	Moment* M_{cr}
DB850-3A	43.84	3376	0.99
DB850-3B	39.53	3297	0.97
DB850-4A	41.71	3580	1.02
DB850-4B	45.81	3664	1.04
DB850-5A	51.80	3567	1.01
DB850-6A	31.33	3509	1.00

Note: 1 kip = 4.448 kN; 1 kip-in. = 0.113 kN-m.
* M_{cr} = 3524 kip-in. for Beams DB850-4, 5, and 6
M_{cr} = 3410 kip-in. for Beam DB850-3
[f'_c = 6000 psi (41.4 MPa), $f_r = 7.5\sqrt{f'_c}$, and f_{se} = 160 ksi (1103 MPa)].

As load increased, the region of cracking expanded. However, the primary region of flexural cracking extended only to about 136 in. (3.45 m) from the end of the beam. At the load of 51.7 kips (230 kN), a flexural crack formed at Station 78, nearly the exact point where debonding is terminated. This also corresponds to the station where initial cracking in the debond/transfer zone is predicted by the behavioral model.

The crack pattern of Test DB850-6A is shown in Fig. 21. In the photograph, the crack at Station 78 is separated from the region of primary cracking by a wide distance. This cracking pattern exemplifies the reduced M_{cr} resulting from debonded strands. End slips coincided with the formation of the crack at Station 78.

DISCUSSION OF RESULTS

Prediction of Cracking

Success of the prediction model is dependent upon the ability to predict the formation of cracks. In Table 5, the first occurrence of flexural cracking is compared to the calculated value. Altogether, there were six test cases. First cracking occurred at moments ranging from a low of 97 percent to a high of 104 percent of the calculated value. The average cracking moment was 100.5 percent of the calculated value, demonstrating very close agreement with the theoretical computation. The cracking moment was calculated based on an effective prestress force of 160 ksi (1100 MPa), a

concrete strength of 6000 psi (41 MPa) and a modulus of rupture equivalent to $7.5\sqrt{f'_c}$. The values for M_{cr} are given in Table 5.

Effects of Cracking on Bond Slip

Table 6 reports the incidence of initial strand slip. In every case, the initial strand slips corresponded with the incidence of cracking through or near the transfer zone of the strands. These results clearly demonstrate that cracking precipitates bond slip. This is an important result, suggesting that bond anchorage can be ensured by designing debonding patterns so that cracking will not affect the debond/transfer zone of pretensioned strands.

For beams with staggered debonding patterns, initial strand slips were caused by flexural cracks at Station 112 (Test DB850-3A), Station 107 (Test DB850-3B), and at Station 108 (Test DB850-4B). For beams with concurrent debonding, strand slips were caused by cracking at Station 80 (Test DB850-5A) and at Station 78 (Test DB850-6A). From Figs. 3 and 5, cracking in the debond/transfer zone should initiate at about Station 103 for beams with staggered debonding patterns, and about Station 78 for beams with concurrent debonding patterns. The test results show that the location of cracking also corresponds very well with the predictions.

Strand Slips and Flexural Failure

In several of the tests, it is noted that small strand slips occurred without complete bond failure. This parallels results found in the literature and also results from the fully bonded development length tests.[3,4,7,12] For example, Specimen DB850-3B, shown in Fig. 17, was able to achieve flexural failure despite 0.28 in. (7.1 mm) of slip on Strand B. Results similar to this were common in tests performed on beams with fully bonded strands.[7,14] Results from these tests and others indicate that strands have the ability to develop the required tension even if some bond slip does occur.

It should also be noted that many of these tests had embedment lengths

Table 6. Summary of strand end slips compared to cracking in the debond/transfer zone.

Test	L_b (in.)	Cracking in the debond/transfer zone		End slips		Mode of failure
		Load at cracking (kips)	Station*	Initial slip	Slip at failure (in.)	
DB850-3A	78(S)	63.44	112	Yes	0.67	Bond
		66.27	88	–		
			96			
DB850-3B	78(S)	66.07	107	Yes	0.28	Flexure
DB850-4A	78(S)	–	–	None	0	Flexure
DB850-4B	78(S)	71.40	108	Yes	0.22	Flexure
		75.11	95	–		
DB850-5A	78(C)	77.78	80	Yes	0.90	Bond
			92	–		
			106			
DB850-6A	78(C)	50.93	78	Yes	0.03	Flexure/Bond

Note: 1 in. = 0.0254 m; 1 kip = 4.448 kN.
* Distance from end of beam (in.).

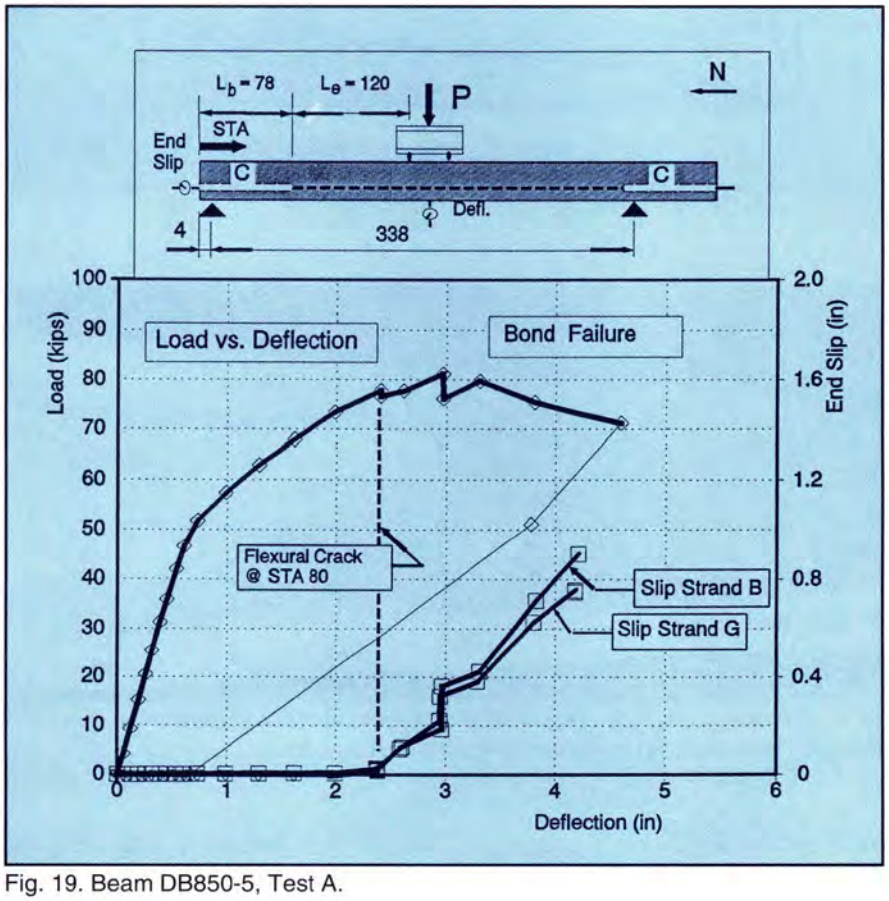

Fig. 19. Beam DB850-5, Test A.

very near the borderline separating expected failure modes. As such, any cracking in the transfer zones occurred at loads very near the nominal capacity and hybrid type failures could be expected. In those cases, the debonded strands may have developed the tension necessary to produce the nominal flexural capacity.

Also, the additional tension required by small increases in flexural load may distribute to the fully bonded strands whose anchorage is unaffected by cracking in the debond/transfer zone. This would explain results from Rabbat et al.[4] and from Dane and

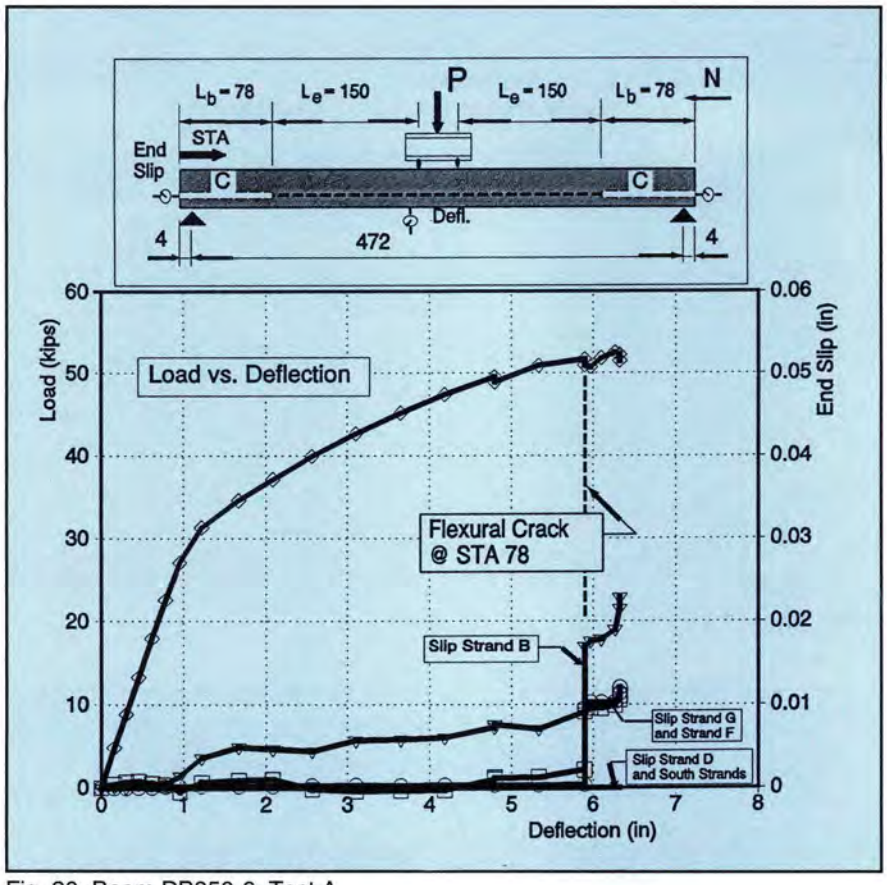

Fig. 20. Beam DB850-6, Test A.

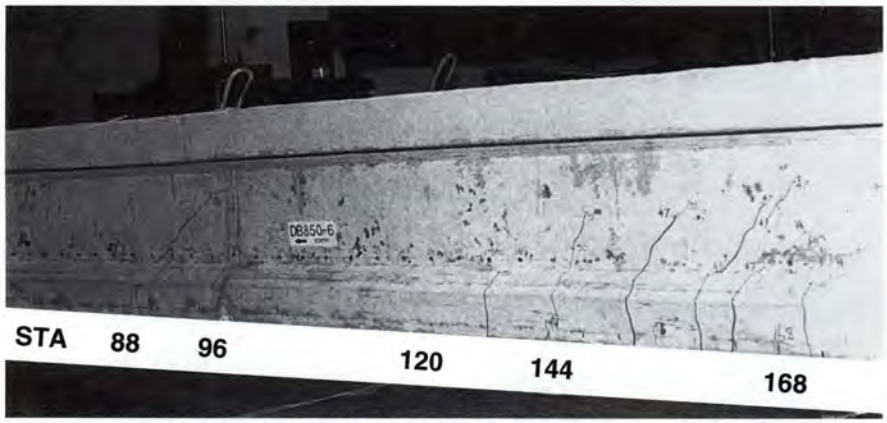

Fig. 21. Cracking pattern for Test DB850-6A depicting crack at Station 78 separated from cracking in regions of maximum moment.

Bruce[12] where significant strand slips were measured, but the beams were able to develop the ultimate load.

Comparison of Results with Predicted Behavior

A model was developed to predict bond failure of pretensioned concrete beams made with debonded strands. The premise for the model is that strand anchorage is likely to fail when cracks propagate through the transfer zone of a strand. By predicting the formation of cracks, bond failure is also predicted.

In Fig. 22, the test results are overlaid on the prediction model of Fig. 7. From the figure, it can be seen that the behavioral model accurately predicts the failure modes of the beams made with debonded strands. For beams with staggered debonding, the behavioral model predicted flexural failure for embedment lengths in excess of 100 in. (2.54 m) and anchorage failures for embedment lengths less than 100 in. (2.54 m).

Of the four tests on beams with staggered debonding, Test DB850-3A, with an embedment length, L_e = 80 in. (2.03 m), failed in bond. The other three tests, Test DB850-3B with L_e = 108 in. (2.74 m), Test DB850-4A with L_e = 120 in. (3.05 m) and Test DB850-4B with L_e = 100 in. (2.54 m), all failed in flexure, as predicted by the behavioral model. Furthermore, the borderline test case (according to the prediction model), Test DB850-4B, suffered significant strand slips with flexural failure, suggesting that shorter embedment lengths would result in bond failure.

For beams with concurrent debonding patterns, the prediction model required an embedment length of 160 in. (4.06 m) to ensure strand development. Test DB850-5A, with L_e = 120 in. (3.05 m), clearly failed in bond, as evidenced by large strand slips and little ductility. On the other hand, Test DB850-6A, with L_e = 150 in. (3.81 m), failed with relatively small strand slips, but lower than expected flexural capacity. Test DB850-6A fell on the borderline between flexural failure and bond failure and the test results verify the borderline behavior predicted by the model. The hybrid nature of this failure is depicted by the solid triangle shown.

Overall, the test results show very close agreement with the prediction model, demonstrating that the prediction of cracking within the debond/transfer zone of a pretensioned strand is an accurate predictor of subsequent failure.

Staggered Debonding vs. Concurrent Debonding

These tests clearly demonstrate that beams with staggered debonding can outperform beams with concurrent debonding. As an example, two tests, DB850-4A and DB850-5A, were constructed with exactly the same debonded length, L_b, and tested to the same embedment length, L_e. However, Beam DB850-4 had staggered debonding while Beam DB850-5 had

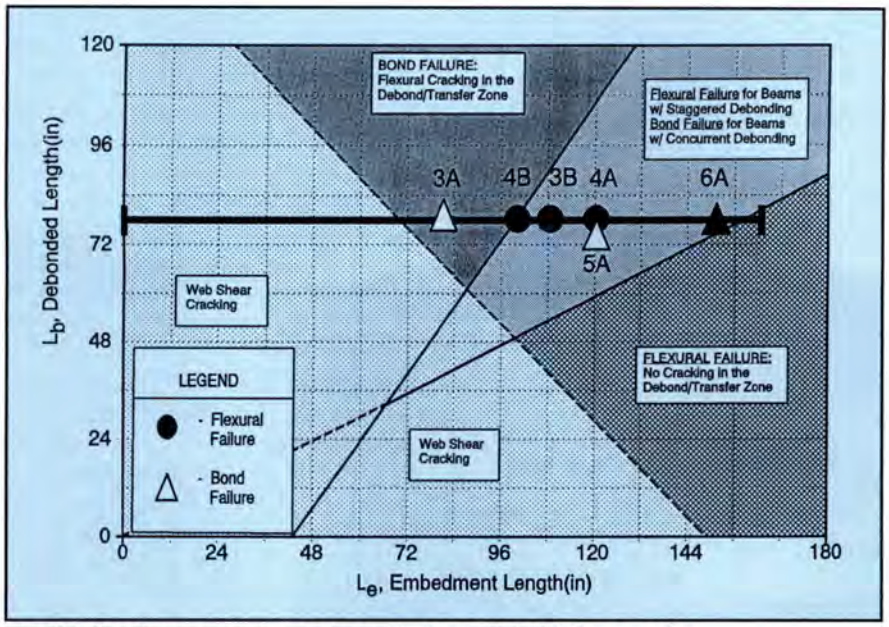

Fig. 22. Overlay comparing test results to predicted failure modes.

concurrent debonding.

Because of staggered debonding, Beam DB850-4 had greater resistance to flexural cracking over most of the debond/transfer zone. As the load increased on Test DB850-5A, the applied moment exceeded M_{cr} at the transfer zone of the debonded strands. Formation of flexural cracks within the debond/transfer zone caused the strands to slip and anchorage was destroyed. As a result, the beam failed in bond.

Conversely, in Test DB850-4A, the applied moment never exceeded M_{cr} in the debond/transfer zone. The beam's ultimate flexural capacity was reached before cracking could occur within the debond/transfer zone. Consequently, the beam failed in flexure. Comparison of these two tests demonstrates that staggered debonding will improve behavior over concurrent debonding, primarily because the beam exhibits greater resistance to cracking.

Comparison to Code Provisions

This research indicates that the current code provisions may be too restrictive in some cases. Many of these tests used embedment lengths that did not conform to the code requirement for twice the basic development length. Yet these strands demonstrated their ability to maintain bond integrity and strand anchorage. The most extreme example is Test DB850-4B. Strands in this specimen demonstrated the bond strength to develop ultimate flexural capacity, yet the embedment length was only 100 in. (2.54 m), not the 160 in. (4.06 m) required by the AASHTO and ACI Codes.

Perhaps more importantly, these test results demonstrate that current code provisions do not establish an accurate model for the behavior of beams with debonded strands. Consequently, current code provisions are, at best, misleading and could result in unsafe designs. The test results do not verify the current code provisions because the embedment length required to prevent bond failure is dependent on factors other than the embedment length of the strand.

These tests also indirectly indicate that current code provisions may allow unsafe designs. For example, consider a simply supported pretensioned girder bridge spanning 100 ft (30.5 m). Current code provisions would require an embedment of 160 in. (4.1 m) and allow debonding to extend to approximately 37 ft (11.3 m) from the support. Clearly, the transfer zone of these debonded strands would be affected by flexural cracking caused by application of large loads. Therefore, such debonded strands may be unable to develop the strand tension required to support ultimate loads. Lower bridge capacity may result.

Fortunately, an accurate prediction of failure mechanisms is possible through the prediction of cracking in the debond/transfer zone. From the prediction model, a safe and reliable design procedure can be developed to ensure the adequate development of debonded prestressing strands. These tests demonstrate that strand development is a function of the beam geometry, the length of debonding, and the pattern of debonding, in addition to the embedment length of the strand.

Furthermore, the behavior of debonded beams can be accurately predicted based on the prediction of cracking in the debond/transfer zone. If a beam is designed so that the debond/transfer zone is unaffected by cracking, then the debonded strands are likely to develop the tension required to develop nominal flexural capacity. For most simply supported beams, flexural cracking in the debond/transfer zone is effectively eliminated if the debond length does not extend from the end of the beam more than 15 percent of the span.

It is important to note the differences in the bond behavior of strands whose debonding is staggered compared with strands whose debonding is concurrent. If strands are concurrently debonded, then the required development length is much greater than if the debonding were staggered. Current code provisions make no distinctions or requirements concerning staggering the debond terminations. This research indicates that staggered debonding should either be required by code language, or better yet, encouraged by code provisions that are more closely related to behavior.

Finally, these tests illustrate that code provisions governing the use of debonded strands should be restructured to reflect the behavior of the beams themselves. These tests clearly demonstrate the relationship between cracking and subsequent bond failures that should be developed into code expressions.

CONCLUSIONS

1. Anchorage failures of debonded strands can be accurately predicted using the behavioral model developed in these tests; anchorage failure is pre-

dicted by the prediction of cracking through the transfer zone of debonded strands.

2. The formation of flexural cracking through the transfer zone of debonded strands causes the affected strands to slip, negatively affecting strand anchorage and leading to bond failure. The result is a loss of prestress and a reduction in the ultimate flexural capacity of the beam.

3. Flexural cracking is predictable based on crack formation at a bottom fiber stress equal to the modulus of rupture, $7.5\sqrt{f'_c}$.

4. Bond failures in beams with debonded strands resulted in ductile failures, even though their nominal capacity is reduced by anchorage failure.

5. Current ACI and AASHTO Code provisions do not adequately reflect behavior and may lead to unsafe designs. Code provisions should be restructured to accurately reflect the relationship between cracking and anchorage failures.

6. The behavior of beams made with debonded strands is predictable and reliable. Therefore, the use of debonded strands should be considered safe, provided the transfer zone of debonded strands is not allowed to extend into regions where cracking will occur at ultimate limit states.

7. In general, staggered debonding should be employed; concurrent debonding may lead to premature anchorage failures. Concurrent debonding results in a lower cracking moment in the debond/transfer zone when compared with staggered cutoff points. Consequently, concurrent debonding can lead to bond failures where staggered debonding will not.

RECOMMENDATIONS

1. Debonded strands may be employed as an alternative to draped strands; however, the debond/transfer zone should not extend into regions of flexural cracking. In simply supported beams, strand debonding should be terminated within 15 percent of the span length, measured from the end of the beam.

2. Debond termination points should be staggered to increase the beam's resistance to cracking in the debond/transfer zone.

3. Code provisions should be restructured to reflect the relationship between cracking and anchorage failures, and to more accurately reflect the behavior of beams made with debonded strands.

ACKNOWLEDGMENT

The research described in this paper was part of a research project sponsored by the U.S. Department of Transportation, Federal Highway Administration, through the Texas Department of Transportation. Their support of the project, "Influence of Debonding of Strands on Behavior of Composite Prestressed Concrete Bridge Girders," is gratefully acknowledged by the authors. The authors also commend Florida Wire and Cable Company for their contribution of prestressing strand.

REFERENCES

1. ACI Committee 318, "Building Code Requirements for Reinforced Concrete (ACI 318-89)," American Concrete Institute, Detroit, MI, 1989.
2. AASHTO, *Standard Specifications for Highway Bridges,* Fourteenth Edition, American Association of State Highway and Transportation Officials, Washington, D.C., 1989.
3. Kaar, Paul H., and Magura, Donald D., "Effect of Strand Blanketing on Performance of Pretensioned Girders," PCI JOURNAL, V. 10, No. 6, December 1965, pp. 20-34.
4. Rabbat, B. G., Kaar, Paul H., Russell, Henry G., and Bruce, Robert N., Jr., "Fatigue Tests of Pretensioned Girders with Blanketed and Draped Strands," PCI JOURNAL, V. 24, No. 4, July-August, 1979, pp. 88-114.
5. Janney, Jack R., "Nature of Bond in Pretensioned Prestressed Concrete," *ACI Journal,* V. 25, May 1954, pp. 717-736.
6. Hanson, Norman W., and Kaar, Paul H., "Flexural Bond Tests of Pretensioned Prestressed Beams," *ACI Journal,* V. 30, January 1959, pp. 783-802.
7. Russell, Bruce W., and Burns, Ned H., "Design Guidelines for Transfer, Development and Debonding of Large Diameter Seven Wire Strands in Pretensioned Concrete Girders," Research Report 1210-5F, Center for Transportation Research, The University of Texas at Austin, Austin, TX, June 1993, 286 pp.
8. ZumBrunnen, Leslie G., Russell, B. W., and Burns, N. H., "Behavior of Statically Loaded Pretensioned Concrete Beams with 0.5 inch Diameter Debonded Strands," Research Report 1210-4, Center for Transportation Research, The University of Texas at Austin, Austin, TX, January 1992, 110 pp.
9. Unay, I. O., Russell, B. W., and Burns, N. H., "Measurement of Transfer Length on Prestressing Strands in Prestressed Concrete Specimens," Research Report 1210-1, Center for Transportation Research, The University of Texas at Austin, Austin, TX, March 1991, 135 pp.
10. Russell, Bruce W., and Burns, Ned H., "Static and Fatigue Behavior of Pretensioned Bridge Girders Made with High Strength Concrete," PCI JOURNAL, V. 38, No. 3, May-June 1993, pp. 118-128.
11. Shahawy, M., and Batchelor, B. deV., "Bond and Shear Behavior of Prestressed AASHTO Type II Beams," Progress Report No. 1, Structural Research Center, Florida Department of Transportation, Tallahassee, FL, February 1991.
12. Dane, John, III, and Bruce, Robert N., Jr., "Elimination of Draped Strands in Prestressed Concrete Girders," Technical Report No. 107, State of Louisiana, June 1975.
13. Horn, Daniel G., and Preston, H. Kent, "Use of Debonded Strands in Pretensioned Bridge Members," PCI JOURNAL, V. 26, No. 4, July-August 1981, pp. 42-58.
14. Lutz, B. A., Russell, B. W., and Burns, N. H., "Measurement of Development Length of 0.5 inch and 0.6 inch Diameter Prestressing Strands in Fully Bonded Concrete Beams," Research Report 1210-3, Center for Transportation Research, The University of Texas at Austin, Austin, TX, February 1992.

APPENDIX — NOTATION

d_b = diameter of prestressing strand

f'_c = specified compressive strength of concrete

f_{ps} = stress in prestressing strand at service load

f_{pu} = stress in prestressing strand at ultimate

f_{se} = effective stress in prestressing strand after prestress losses

L_b = debonded length of prestressing strand

L_d = development length of prestressing strand

L_e = embedment length of prestressing strand

L_t = transfer length of prestressing strand

M_{cr} = cracking moment of beam

M_n = moment of beam at service load

M_u = maximum moment of beam at failure

P_u = ultimate load of beam

S_b = section modulus of beam

V_{cw} = shear strength of beam to resist web cracking